Spatially precise activation of the mouse cochlea with a multi-channel hybrid cochlear implant

Journal of Neural Engineering

PAPER

Spatially precise activation of the mouse cochlea with a multi-channel hybrid cochlear implant

Ajmal A Azees[1,2], Alex C Thompson[1,11], Patrick Ruther[3,4], Elise A Ajay[1,5], Jenny Zhou[1], Ulises A Aregueta Robles[6], David J Garrett[2], Anita Quigley[2,7,8,9], James B Fallon[1,10,11] and Rachael T Richardson[1,11,*]

[1] The Bionics Institute, Fitzroy, VIC 3065, Australia
[2] Department of Biomedical Engineering, RMIT University, Melbourne, VIC 3000, Australia
[3] Department of Microsystems Engineering (IMTEK), University of Freiburg, 79110 Freiburg, Germany
[4] BrainLinks-BrainTools Center, University of Freiburg, 79110 Freiburg, Germany
[5] Faculty of Engineering and Information Technology, University of Melbourne, Melbourne, VIC, Australia
[6] Graduate School of Biomedical Engineering, University of New South Wales, Sydney, NSW 2033, Australia
[7] St Vincent's Hospital Melbourne, Aikenhead Centre for Medical Discovery, Fitzroy, Melbourne, VIC 3065, Australia
[8] St. Vincent's Hospital Melbourne, Centre for Clinical Neurosciences and Neurological Research, Fitzroy, Melbourne, VIC 3065, Australia
[9] Department of Medicine, St Vincent's Hospital Melbourne, The University of Melbourne, Fitzroy, Melbourne, VIC 3065, Australia
[10] Department of Surgery (Otolaryngology), University of Melbourne, The Royal Victorian Eye and Ear Hospital, East Melbourne, VIC 3002, Australia
[11] Medical Bionics Department, University of Melbourne, East Melbourne, VIC, Australia
[*] Author to whom any correspondence should be addressed.

E-mail: rrichardson@bionicsinstitute.org

Keywords: cochlear implant, optogenetics, electrical stimulation, hybrid, inferior colliculus, channel interference

OPEN ACCESS

RECEIVED
1 November 2024

REVISED
9 April 2025

ACCEPTED FOR PUBLICATION
24 April 2025

PUBLISHED
6 May 2025

Abstract

Objective. Cochlear implants are among the few clinical interventions for people with severe or profound hearing loss. However, current spread during monopolar electrical stimulation results in poor spectral resolution, prompting the exploration of optical stimulation as an alternative approach. Enabled by introducing light-sensitive ion channels into auditory neurons (optogenetics), optical stimulation has been shown to activate a more discrete neural area with minimal overlap between each frequency channel during simultaneous stimulation. However, the utility of optogenetic approaches is uncertain due to the low fidelity of responses to light and high-power requirements compared to electrical stimulation. *Approach.* Hybrid stimulation, combining sub-threshold electrical and optical pulses, has been shown to improve fidelity and use less light, but the impact on spread of activation and channel summation using a translatable, multi-channel hybrid implant is unknown. This study examined these factors during single channel and simultaneous multi-channel hybrid stimulation in transgenic mice expressing the ChR2/H134R opsin. Acutely deafened mice were implanted with a hybrid cochlear array containing alternating light emitting diodes and platinum electrode rings. Spiking activity in the inferior colliculus was recorded during electrical-only or hybrid stimulation in which optical and electrical stimuli were both at sub-threshold intensities. Thresholds, spread of activation, and threshold shifts during simultaneous hybrid stimulation were compared to electrical-only stimulation. *Main results.* The electrical current required to reach activation threshold during hybrid stimulation was reduced by 7.3 dB compared to electrical-only stimulation ($p < 0.001$). The activation width measured at two levels of discrimination above threshold and channel summation during simultaneous hybrid stimulation were significantly lower compared to electrical-only stimulation ($p < 0.05$), but there was no spatial advantage of hybrid stimulation at higher electrical

stimulation levels. *Significance.* Reduced channel interaction would facilitate multi-channel simultaneous stimulation, thereby enhancing the perception of temporal fine structure which is crucial for music and speech in noise.

1. Introduction

According to the World Health Organization, over 1.5 billion people live with hearing loss, with 430 million individuals having a hearing loss greater than 35 decibels (dB) in the better hearing ear (WHO 2021). Cochlear implants can be used to evoke hearing perception by electrically stimulating spiral ganglion neurons in the inner ear, emulating to some extent the input provided by sensorineural hair cells in an unimpaired cochlea (Wilson and Dorman 2008). However, cochlear implants are still far from restoring normal hearing. Ideally, each electrode should activate different regions of the cochlea, corresponding to different frequencies of sound. However, electrical stimulation across different electrodes activates overlapping regions of the cochlea due to current spread in the highly conductive perilymphatic fluid (Black *et al* 1981, Snyder *et al* 2004, Bierer 2007, George *et al* 2015, Quass *et al* 2024). If electrodes were to be stimulated simultaneously, the channel summation that would occur in the overlapping regions would cause uncontrolled loudness (Marozeau *et al* 2015). Clinically, channel summation is mitigated by interleaved pulsed stimulation strategies, but at the expense of more natural sound encoding across different frequencies. Currently, cochlear implant users experience poor speech discrimination in noisy environments (Fu *et al* 1998, 2005, Shannon *et al* 2004) and poor music perception (McDermott 2004, Gfeller *et al* 2007). Even in quiet settings, speech intelligibility is still compromised for tonal languages such as Mandarin (Huang *et al* 2005) and for pitch-accent languages like Persian (Poursoroush *et al* 2015).

To date, most commercialised cochlear implants use a monopolar (MP) electrode configuration to stimulate spiral ganglion neurons despite the well-known problem of current spread (Bierer *et al* 2002, Snyder *et al* 2004). Several other stimulation configurations have been explored to focus the stimulation, such as bipolar, tripolar, focussed multipolar and common ground (CG), all demonstrating more focused neural activation in the cochlea compared to MP stimulation (Shannon 1983, Kral *et al* 1998, Bierer *et al* 2004, George *et al* 2014). Despite the theoretical expectation and pre-clinical evidence of reduced activation spread, psychophysical and speech recognition measurements in clinical studies showed variable, similar or, in some cases, worse performance of bipolar or other focused stimulation modes compared to the MP mode (Lehnhardt *et al* 1992, Zwolan *et al* 1996, Pfingst *et al* 1997, 2001, Mens *et al* 2005, Berenstein *et al* 2008, Srinivasan *et al* 2013, Fielden *et al* 2015). The lack of clear clinical benefit of current focusing techniques may be partly because the stimulating current at speech comfort levels is higher for the focussed configurations compared to MP stimulation, which would override the advantages of the sharper electrical field at near-threshold currents.

Optical stimulation is an alternative method of neuromodulation that has the potential to provide higher spectral resolution compared to electrical stimulation, even at higher stimulating intensities. Light in the infrared wavelengths is proposed to activate spiral ganglion neurons through a heat-based mechanism (Albert *et al* 2012), while visible light can activate spiral ganglion neurons only after modifying the neurons with optogenetic actuators called opsins (Deisseroth 2011, 2015, Fenno *et al* 2011). For optogenetic stimulation, light can be applied to the cochlea via optical fibres or implanted light-emitting diodes (LEDs) (Huet *et al* 2024). *In vivo* studies have shown that optogenetic stimulation using LEDs provides greater spectral resolution as compared to electrical stimulation (Hernandez *et al* 2014, Wrobel *et al* 2018, Dieter *et al* 2019, 2020b, Keppeler *et al* 2020), creating independent frequency 'channels' that produce minimal interference on other channels, even when simultaneously stimulating neighbouring LEDs (Azees *et al* 2023). Modelling studies in non-human primates and human cochleae also predict spatially restricted activation of spiral ganglion neurons using LEDs or waveguides (Jürgens *et al* 2018, Keppeler *et al* 2021, Khurana *et al* 2022), providing support to the translational potential of optical cochlear implants.

Significant advances in the translation of optogenetic techniques for hearing restoration include the genetic modification of the spiral ganglion neurons (Zhang *et al* 2018, Crane *et al* 2021, Yoshimura *et al* 2021, Qi *et al* 2022, Zerche *et al* 2023), development of optical cochlear implants (Wrobel *et al* 2018, Dombrowski *et al* 2019, Klein *et al* 2019, Keppeler *et al* 2020, Dieter *et al* 2020a, 2020b, Helke *et al* 2022, Moser 2022), and speech processing strategies (Khurana *et al* 2023). However, a critical challenge for successful translation of optogenetic stimulation into the clinic is the limited temporal response of opsin channels (Thompson *et al* 2020, Ajay *et al* 2023, Mittring *et al* 2023). Even for the fastest available

opsins, Chronos-ES/TS and f-Chrimson, mean spiking probability was 50% for 150 Hz stimulation (Keppeler *et al* 2018, Mager *et al* 2018), which is at the lower end for providing sufficient temporal cues for speech understanding (Fu *et al* 2000, Fu 2002), with 300–500 Hz being more typical of the stimulation rates used in commercial cochlear implants.

An approach that combines electrical and optogenetic stimulation has been explored to exploit the high temporal resolution offered by electrical stimulation and the spectral resolution of optical stimulation. The premise of combined electrical and optogenetic stimulation is that focused optical stimulation raises the resting membrane potential of neurons in a confined region of the cochlea to near-threshold (below auditory perception) while the addition of sub threshold electrical stimulation causes the 'primed' nerve cells to fire, thereby evoking a hearing percept. Through this facilitation, less electrical current is required to produce spiking activity in the region of the light, thereby resulting in a sharper spatial tuning curve compared to electrical stimulation alone (Duke *et al* 2009, 2012b, Thompson *et al* 2020). Using acutely deafened mice that expressed the ChR2-H134R opsin, a well-characterised variant of ChR2 with higher light sensitivity and slightly slower closing kinetics (Lin 2011), Thompson *et al* showed a 2.4-fold increase in the maximum frequency following rate during single channel hybrid stimulation compared to optogenetic-only stimulation (2020). Ajay *et al* also demonstrated that temporal fidelity and precision could be increased with hybrid stimulation in acutely- and chronically deafened transgenic mice expressing ChR2-H134R opsin, via auditory nerve recordings (2023, 2024). In these cases, hybrid stimulation was delivered via a laser-coupled optical fibre and 25 μm platinum/iridium wire, both inserted through the round window (RW) membrane, thus not being representative of a clinically translatable array.

In the present study, we investigated hybrid stimulation using an array consisting of multiple alternating platinum electrodes and LEDs miniaturised for the mouse cochlea, with the electrodes modelled off a human cochlear implant to ultimately enhance translatability. The objectives were to examine the spread of activation during single channel stimulation and channel summation during two-channel simultaneous stimulation, measured via the extent and threshold of spiking activity in the inferior colliculus (ICs) of the auditory midbrain. Hybrid stimuli consisted of sub-threshold optical stimuli and a range of electrical current levels (CL). Experiments were conducted using transgenic mice expressing the ChR2-H134R opsin in all spiral ganglion neurons. The research findings highlight the potential and limitations of hybrid stimulation to independently stimulate two channels simultaneously, which could allow enhanced encoding of complex speech signals as well as the fine changes in the timing information of speech.

2. Methods

2.1. Hybrid stimulating arrays

Hybrid stimulating arrays for the mouse cochlea were designed and fabricated for this study, integrating LEDs (270 × 220 μm) into an array of five platinum electrode rings. Modelled from the human cochlear implant, the mouse electrical arrays have tapering platinum electrodes in a soft silicone carrier. Standalone arrays of the LEDs used for the hybrid device have been validated in a previous study (Azees *et al* 2023).

2.1.1. Micro-CT scans

Micro-CT scans were conducted using a Bruker micro-CT scanner (Skyscan 1276). A formalin fixed (10% V/V neutral buffered formalin) dissected mouse cochlea, with or without an inserted array, was transferred to an Eppendorf tube filled with phosphate-buffered saline. The sample was placed on a 12 mm sample bed (smallest pixel size of 2.8 μm). Scanning settings of 0.2-degree steps, 360 degrees and the 3-frame average were used to scan the cochlea. Images were reconstructed using the NRecon (Bruker software) and CTVox software.

2.1.2. LED fabrication and parylene C coating

Arrays of 5 LEDs (453 nm wavelength; CREE C460TR2227, CREE, Durham, USA) were assembled on a 10 μm-thin polyimide substrate in a clean room facility, as described previously (Azees *et al* 2023). The light-emitting area of each LED was 270 × 220 μm. LED arrays were cleaned in isopropanol solution and then soft baked at 80 °C for 1 h in a laboratory oven (Dehydrating oven, LABEC). Then, oxygen plasma (HPT-100, Princeton Scientific Corporation) was applied for 1 min on each side of the LED array to increase adhesion properties between the LED array and parylene C. Then, using the vapour deposition polymerisation method, a parylene C coating was applied to the LED arrays (PDS 2010, Specialty Coating Systems) by running the parylene coating machine twice without taking the LED arrays out from the machine. Four grams of parylene C was used for each run and the total thickness of the parylene coating was estimated to be 5 μm.

2.1.3. Silicone mould coating and addition of electrodes

The addition of electrodes and silicone mould coating process were performed in a clean room facility. Five platinum rings (200 μm width) with tapering diameters (0.29, 0.27, 0.25,0.23, 0.21 mm) were

used. Each ring was cut and opened into a cup-shape to allow the LEDs to be placed into the array. Platinum wire (25 μm diameter) was laser-welded to the electrode to form electrical connection. These electrodes were carefully placed into a mould, ensuring the openings faced upwards and their diameters increased sequentially from tip to base. The parylene C-coated LED array was gently positioned within the electrodes to achieve alternating LEDs and electrodes. Medical-grade silicone (MED 4860) was then injected to encapsulate the electrodes, followed by curing (120 °C for one hour) and demolding. Any excess material was removed from the platinum rings using a scalpel. To achieve a rounded tip, a small amount of MED 4210 silicone was applied to the end of the array, utilising the surface tension during the curing process to form a desired hemispherical shape. The assembled hybrid array underwent an additional curing process in the oven at 120 °C for 15 min. The length of the hybrid array was 2.76 mm from the tip to the base LED. The inter-LED pitch and inter-electrode pitch (centre-to-centre) was 520 μm.

The gold conducting lines from LEDs and the coiled lead wires from electrodes were soldered to a custom designed printed circuit board, which had connector pins for connection to bench top stimulators.

2.1.4. Integrity tests and characterisation of arrays

The impedance, integrity of coatings and mechanical properties of all arrays were tested prior to use in animal experiments.

Impedance was measured before and after soaking the arrays in warm saline solution (37 °C) for up to 24 h. Impedance was also measured before and after bending the cochlear implant array around a 1 mm diameter metal rod and/or insertion in a 3D printed model of a mouse tympanic duct (see Artificial mouse scala tympani model). MP return impedance and CG impedance measurements were used to diagnose the functionality of individual electrodes and LEDs.

A photodiode was used to compare the output power before and after parylene C coating. The photodiode was positioned 8 mm above the surface of the LED as dictated by the physical constraints of the inbuilt photodiode enclosure. The photodiode was moved horizontally during measurements to measure the extent of the beam.

A power meter (LP10, Sanwa) was used to measure the peak surface output power of LEDs to determine the relationship between input-current and output-power. The power meter was calibrated for the wavelength of the LED and the light sensor of the power meter was positioned just above the illuminating LED to ensure precise measurements. Input current was given in steps of 0.2 mA up to 2 mA and thereafter 0.5 mA steps.

2.1.5. Artificial mouse scala tympani model

3D-printed models of the mouse cochlea scala tympani lumen were made using in-house made hydrogel bioinks following reported procedures (Aregueta Robles *et al* 2023). The dimensions were obtained from micro-CT scans of the mouse cochlea, processed with open-source software 3D Slicer (www.slicer.org). These measurements were used for creating a custom-lofted spiral in SolidWorks (Dassault Systèmes SolidWorks Corporation), which served as a negative template for the final digital model. For visualisation purposes, the model was truncated to present an open channel representing the first turn from the RW. The bioink consisted of methacrylated poly(vinyl alcohol) (PVA-MA, 20 wt%), supplemented with lithium phenyl-2,4,6-trimethylbenzoylphosphinate (photo-initiator, 0.8 wt%), and tartrazine (photo-absorber, 1 m ml^{-1}). The model was fabricated using a LumenX+ 3D printer (Cellink, Sweden) at a resolution of 50 μm, 3 s of light exposure per layer at 20 mW cm^{-2}.

2.2. Animals and ethics approval

The hybrid stimulation experiments used heterozygous transgenic mice generated from a cross between Cre-parvalbumin mice (B6;129P2-Pvalb$^{tm1(cre)Arbr}$, Jax strain 008069) and COP4-H134R/EYFP mice (B6;129SGt(ROSA)26Sor$^{tm32(CAG\ COP4*H134R/EYFP)Hze/J}$, Jax strain 012569, backcrossed onto a C57BL/6 background). These mice have been previously characterised to express the H134R variant of channelrhodopsin-2 in all spiral ganglion neurons, as well as inner hair cells and outer hair cells of the cochlea (Thompson *et al* 2020). Four male mice and four female mice were used in this study at 7–12 weeks of age. Approval for the use and care of the experimental animals in this research was granted by the St Vincent's Hospital Animal Ethics Committee in Melbourne, Australia (#21–007), in accordance with the Guidelines to Promote the Wellbeing of Animals used for Scientific Purposes (2013), the National Health and Medical Research Council Code for Care and Use of Animals for Scientific Purposes (8th edition, 2013), and the Prevention of Cruelty to Animals Amendment Act (2015).

2.3. Anaesthesia, analgesia, and monitoring

Mice were anesthetised with isoflurane for implantation and recordings. Respiration and depth of anaesthesia were regularly monitored, and a heating pad was used to maintain the body temperature at 37 °C. Local anaesthesia (0.5% Marcaine, s.c.) was administered at the wound margins of the surgical sites.

2.4. Surgical exposures and insertion of stimulating/recording electrodes

The cochlea was surgically exposed using standard methods (Stevens *et al* 2015) to deafen the mouse and allow insertion of the hybrid stimulating array.

After drilling through the bulla to expose the cochlea, a cochleostomy was made in the mid-apical turn of the cochlea and the RW membrane was punctured using a fine borosilicate pipette. Five microlitres of neomycin sulphate (10%, w/v) in saline was injected over a period of 20 min. The cochlear surgical site was temporarily plugged with saline-moistened cotton wool while the recording site in the brain was surgically exposed. A craniotomy and durotomy were made near the intersection of the parietal and interparietal bones contralateral to the deafened cochlea to expose ICs of the auditory midbrain. Saline was added to the surgical site to prevent drying while the multichannel hybrid array was inserted into the cochlea through the RW. The array was inserted to a depth of 2 hybrid channels (2 electrodes and 2 LEDs) to safeguard against potential damage to the cochlea or array during the insertion process. A 32 channel multi-channel recording array (NeuroNexus Technologies, MI, USA) with 50 μm inter-electrode spacing was inserted vertically into the ICs of the midbrain to a depth of approximately 1750 μm using a Microdrive positioner (David Kopf Instruments, USA). Responses to optical or electrical stimuli for the tip electrode of the hybrid array were monitored on a raster plot to determine insertion depth, ensuring the recording array was accurately placed within the central nucleus of the ICs. Recordings commenced approximately 5 min after the insertion of recording electrode, allowing time for the brain to settle and stabilise after the insertion process. Agar solution was applied 1% (w/v) to the surface of the ICs and around the recording array to enhance stability of recordings and to provide electrical contact of the internal reference electrode with the brain.

2.5. Optical, electrical, and hybrid stimuli

All stimuli were presented at 4 Hz to study single pulse responses and were controlled by custom software executed in Igor Pro (Wavemetrics, Portland, OR). Each set of stimuli was presented 10 times in a randomised order.

2.5.1. Optical stimuli

The threshold for optical activation was determined individually for each LED and for each mouse, where threshold was defined as the lowest intensity level which elicited 30% of maximum spikes. This was achieved by driving the LEDs at 0–10 mA (0–3.4 mW) by an in-house custom-built LED driver. The optical pulses were 1 ms in duration. Optical threshold was re-checked at the conclusion of each experiment and was confirmed to be stable over time.

2.5.2. Electrical stimuli

Cathodic-first MP biphasic pulses of 25 μs/phase (8 μs interphase gap) were delivered through the platinum bands of the hybrid array. An extracochlear stainless-steel 23-gauge needle placed subcutaneously in the left side axillary region of the mouse served as the return electrode. A custom-built in-house multichannel stimulator was used to generate the stimulus waveforms. The amplitude of the electrical current was expressed in CL, representing the amplitude of biphasic pulses on a logarithmic scale similar to the decibel scale of acoustic power, where current in μA is provided by: $I = 17.5 \times 100^{\frac{CL}{255}}$. The electrical stimuli were delivered to each electrode between 0 and 260 CL or if myogenic activity was present (visual observation of muscle twitches), the maximum stimulating current was capped at 10 CL below the myogenic level.

2.5.3. Hybrid stimuli

The hybrid stimulation consisted of an electrical pulse delivered 1.5 ms after the onset of the optical pulse. This delay was previously shown to yield an optimal facilitation of the neural response, as measured by the reduction in the electrical threshold and response reliability (Thompson *et al* 2020). A hybrid channel was defined as a combination of a single LED and an adjacent platinum band electrode. Therefore, hybrid channel H4 was a combination of L4 and E4, and hybrid channel H5 was a combination of L5 and E5. The optical intensity for L4 and L5 used in hybrid stimulation was used at a sub-threshold level (40%–90% of the optical threshold, determined individually for each mouse), while the electrical stimulation was delivered at the full range of CL (up to 260 CL or the myogenic limit).

2.5.4. Hybrid interference study

This experiment employed an interference protocol where two channels, the more basal interference channel (H4) and the more apical test channel (H5), were stimulated simultaneously. Using the established sub-threshold optical intensity for H4 (See Hybrid stimuli), the E4 electrical current that yielded threshold activity was determined for each individual mouse so that it could be set to four different stimulus levels (10 CL below threshold, at threshold, 10 CL above threshold, and 20 CL above threshold) for the interference study. At the same time, the H5 test channel was stimulated over the full current range (up to 260 CL) in steps of 10 CL, along with its established optical threshold intensity.

The interference study was only performed for hybrid stimulation. An electrical stimulation interference study could not be performed within this cohort of mice due to time and ethical considerations, since conducting the hybrid stimulation acute experiment alone required more than 12 h of anaesthesia per mouse. A study on electrical interference was performed previously using an identical setup and an electrode array of very similar design (Azees *et al* 2023). Therefore, wherever relevant, the results of the hybrid interference study have been compared to our published data.

2.6. Response data analysis

Multi-unit spike activity from all 32 recording electrodes was amplified, filtered, and digitised at a sample rate of 30 kHz using a Cerebus data acquisition system (Blackrock Microsystems, USA). Customised spike detection scripts in Igor Pro (Wavemetrics, Portland, OR) were used to process multi-unit activity. Electrical stimulus artifacts were removed using methods outlined in Heffer and Fallon (Heffer *et al* 2008). Spikes were detected at four times the root mean square for threshold crossings on each recording channel. Spikes were counted during a 5–40 ms post-stimulus window for stimulus artifact removal and to capture all possible responses of ICs neurons to optical, electrical, and hybrid stimulation. Spike counts across the multi-unit recording array were used to generate response images, with the recording electrode number on the X-axis and the stimulus intensity on the Y-axis and the neural response strength colour coded to show total number of spikes in the analysis window. The threshold was defined as per the Hybrid Stimuli section and the threshold of each recording electrode was connected to generate a spatial tuning curve. The recording electrode with the lowest threshold was identified as the best recording electrode. If this amounted to more than one, then of these electrodes, the one with the highest spiking activity was used.

2.6.1. Spread of activation

The discrimination index (d′) (Green *et al* 1973), was used to quantify the growth in neural response with increasing stimulus intensity at each recording location. The widths of the spatial tuning curves were measured at two supra-threshold levels (cumulative $d' = 1$ and $d' = 2$ above threshold) and at each stimulating current level for cross-modality comparison.

2.6.2. Channel interaction and threshold shift

Input–output curves were generated for the best recording electrode for single channel stimulation and simultaneous stimulation. The threshold shift for the test channel and relative threshold influence were calculated from the input–output curves as described previously (George *et al* 2015, Azees *et al* 2023).

2.7. Statistical analysis

The Shapiro–Wilk test was used to assess the normality of all data. The equivalence of variance was examined using the Brown–Forsythe method. Two-way analysis of variance (ANOVA) on Ranks (stimulus type x channel) was conducted to compare the spread of activation calculated at $d' = 1$ and $d' = 2$ above the threshold during the electrical stimulation and hybrid stimulation and followed by the Holm-Sidak post hoc analysis. The criterion for statistical significance was set at a significance level of $p < 0.05$. Separate paired t-tests were conducted to compare the statistical significance between the electrical threshold and hybrid threshold for the channels H4 and H5. A paired t-test was performed to compare the relative reduction of electrical threshold percentage between the different channels.

3. Results

3.1. Developing hybrid arrays for the mouse cochlea

3.1.1. Output power of LEDs

The relationship between input-current to output-power was determined for 3 bare LEDs, each measurement taken with the photodiode centred over the LED. The peak output power increased linearly with the input current (equation (1), figure 1(A)).

$$\text{Output power (mW)} = \frac{343.37 * \text{Input current (mA)} - 41.914}{1000}. \quad (1)$$

A biocompatible protective coating is essential to the incorporation of LEDs into medical devices to protect the device from bodily fluids and to protect the body from electrical charges. The output power of the LEDs was assessed before and after applying the parylene C coating to the LED array. The 5 μm layer of parylene C coating did not result in any significant variations in the output power (figure 1(B)).

3.1.2. Thin film LED array component

The parylene-coated LED array component of the hybrid cochlear implant prototypes passed all bending and 24 hour saline soak tests, with no change in impedance after bending or soaking. A micro-CT scan revealed that an encapsulated and silicone-coated LED array could be fully inserted into an extracted mouse cochlea via the RW and bend appropriately with the cochlear turns, meeting the required flexibility and size requirements for further development into hybrid arrays (figure 1(C)).

3.1.3. Hybrid arrays

All prototype hybrid arrays passed the bending and saline soak tests. Despite this, fully implanted hybrid arrays exhibited failures during *in vivo* implantations. Since this was not the case for the LED-only array (Azees *et al* 2023), a property of the hybrid array was hypothesized to be causing the failure. To understand the source of failure, we inserted a hybrid array into a PVA-based 3D-printed hydrogel model of the cochlear basal turn tympanic duct using the dimensions extracted from a micro-CT scan of a mouse cochlea. This allowed us to observe the bending of the array during insertion and its final inserted position *in situ*. During the insertion of the hybrid electrode, we observed that it was not easily bending around the cochlear turn and was causing damage to the sides of the 3D-printed cochlear duct (figure 1(D)). Of note,

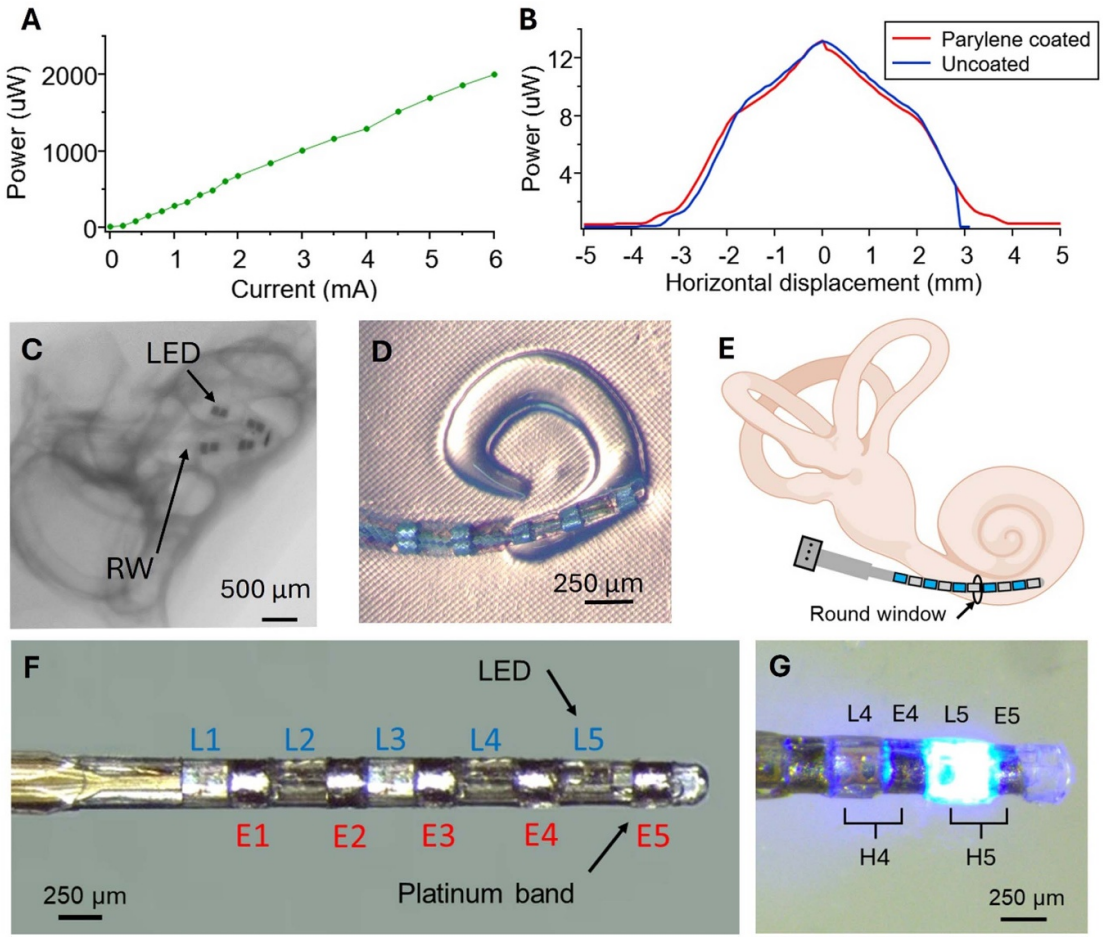

Figure 1. Optical-only and hybrid array testing. (A) The peak output power of a light-emitting diode (LED) using a 1 ms pulse duration increased linearly with stimulating current. (B) The average output power of LEDs (5 mA stimulating current, $n = 3$) showed little difference before parylene coating (blue) and after parylene coating (red). The power was measured at different horizontal displacement of photodiode. (C) A Micro-computed tomography scan image showing an extracted cochlea with an implanted array of 5 LEDs. Arrowheads are pointing to the LEDs fully implanted inside the cochlea and the round window (RW). (D) A hybrid cochlear implant inserted into a 3D printed cochlea (polyvinyl alcohol) showing the extent of insertion prior to impacting the wall of the cochlear duct. (E) Schematic showing the implantation of a hybrid array in the mouse cochlea, with two LEDs (blue) and two electrodes (grey) inserted. Image created in BioRender.com. (F) Hybrid array for the mouse cochlea. Five 270 × 220 μm LEDs ($\lambda = 453$ nm; labelled L1–L5) and five 200 μm-wide platinum bands (labelled E1–E5), tapering in diameter from 290 μm to 210 μm and arranged in an alternating pattern in a silicone carrier. (G) Hybrid array with tip LED (L5) operating. The combined operation of L4 and E4 is referred to as a hybrid channel, labelled as H4. Likewise, the combination of L5 and E5 form another hybrid channel (H5).

this hydrogel technology has been proven to handle the implantation of human cochlear electrode arrays. It has also been tested to withstand up to 8 N of compression load and 50% strain without impacting on the structure and strength (Aregueta Robles *et al* 2023). Although it was possible to fully insert the hybrid array in the cochlea, the increased size and stiffness of the hybrid array compared to the LED-only array was causing mechanical damage to the gold conducting lines of the LEDs during full insertion. Subsequent experiments were performed in which the insertion was limited to two electrical channels and two optical channels (two hybrid channels; H4 and H5) (figure 1(E)). With this approach, a single hybrid array was successfully used during eight acute hybrid stimulation experiments and remained undamaged and fully functional (figures 1(F) and (G)).

3.2. Hybrid optical and electrical stimulation reduces electrical threshold

Single channel electrical-only and optical-only stimulation was conducted for hybrid channels 4 and 5 of the array in each mouse. During stimulation, spiking activity in the ICs of the auditory midbrain was recorded across the 32 channels of the recording array, where electrode 32 is the deepest recording electrode (corresponding to the basal region of the cochlea). The best recording electrode (electrode with the lowest threshold) of each modality was determined. When stimulating with the most apically inserted channel in the cochlea (E5), the best recording electrode was on a more superficial recording electrode (figure 2(A)). The best recording electrodes for L5, E4, and L4 were recorded on increasingly deeper recording electrodes of the ICs, in accordance with

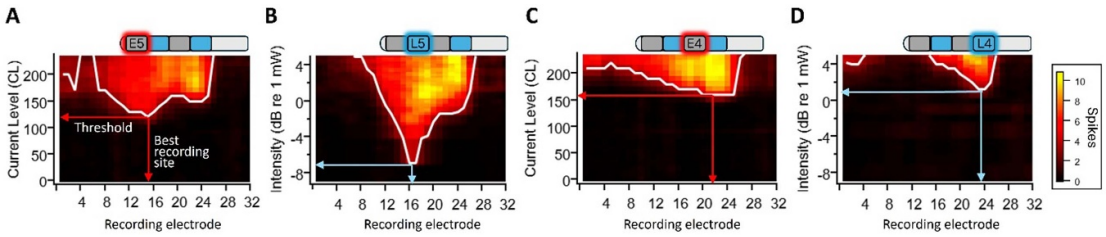

Figure 2. Response images to electrical-only and optical-only stimulation of the cochlea. Representative response images from one animal to electrical or optical stimulation on electrode 5 (E5) (A), LED 5 (L5) (B), electrode 4 (E4) (C), and LED 4 (L4) (D), as indicated by the schematic of the hybrid array. For each response image, the recording electrode was numbered from 1 to 32, with electrode 1 corresponding to the most superficial recording electrode (low frequency region of the inferior colliculus (IC), apex of the cochlea) and electrode 32 to the most deeply inserted electrode (high frequency region of the IC, base of the cochlea). Best recording electrodes and thresholds are indicated on each image (red/blue arrows), demonstrating that shifting the cochlear stimulation site from the most apically inserted E5 to the most basally positioned channel L4 corresponds to a shift from a superficial best recording site in the inferior colliculus (IC) to a deeper best recording site in the IC. The white lines are the spatial tuning curves, indicative of 30% of maximum spiking activity for each recording electrode.

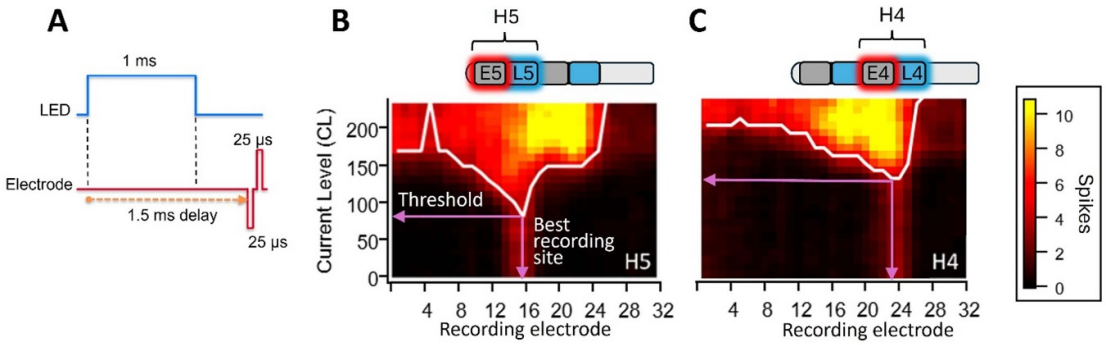

Figure 3. Hybrid stimulation of the cochlea. (A) Schematic of the hybrid stimulus, comprising an optical pulse (1 ms) from a light-emitting diode (LED) and an electrical pulse (25 μs/phase biphasic current pulse with an interphase gap of 8 μs). The electrical pulse was delayed by 1.5 ms relative to the onset of the optical pulse. (B)–(C) Response images to hybrid stimulation (with 75% optical intensity) on hybrid channels 5 and 4 (H5 and H4), respectively (same animal as in figure 2, showing an intermediate best recording site and reduction in threshold for both channels compared to electrical-only stimulation). Response images are as described in figure 2.

their more basal position in the cochlea (figures 2(B)–(D)). The optical thresholds for L4 and L5 were used to set the optical intensity level for the hybrid stimulus for each animal, while changes in the electrical threshold were used to measure response facilitation during hybrid stimulation.

Example response images to stimulation of hybrid channel 4 (H4) and hybrid channel 5 (H5) are shown in figure 3 (same animal as used in figure 2), where the optical stimulus was set to 75% of threshold while a full range of electrical currents was applied. These images show a reduction in threshold and a small shift in best recording electrode compared to electrical-only stimulation shown in figures 2(A) and (C). In addition, just like the individual electrical and optical modalities, the best recording electrode for H4 resulted in spiking activity that was more basal in origin compared to H5.

To determine the effective range of light stimulus intensities that resulted in facilitation of the electrical stimulus, a series of hybrid stimulation protocols were run, holding the optical stimulus at various sub-threshold levels (40%–90% of optical threshold) while applying a full range of electrical CL. In the example shown in figure 4(A), when optical stimulation was applied at 60% of threshold, the electrical threshold during the hybrid stimulus was unchanged compared to the electrical-only stimulus (both determined at the best recording site for the electrical-only stimulus). However, when the optical stimulus was applied at 75% of optical threshold or above, hybrid stimulation caused a localised reduction in electrical threshold compared to the electrical-only stimulus. Figure 4(B) shows the effect of different sub-threshold light intensities on the electrical threshold for all mice in the study, measured on the best electrode identified during electrical-only stimulation.

The hybrid stimulation parameters used for subsequent experiments were based on the optical intensity that resulted in response facilitation (approximately mid-way way between no facilitation and lowest threshold recorded). Based on this definition, the optical intensities used ranged from 45%–90% of

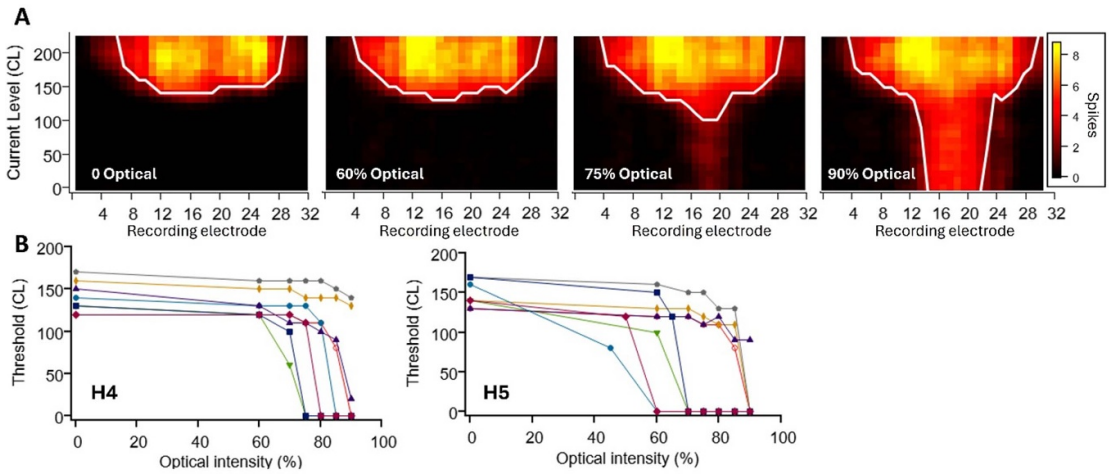

Figure 4. Effect of optical intensity on hybrid stimulation responses. (A) Example response images from one animal to hybrid stimulation on hybrid channel 5 (H5) with different sub-threshold optical intensity levels. In these examples, the optical pulse was delivered at 0% (i.e. only electrical stimulation was applied) and at 60%, 75%, and 90% of the optical threshold, as indicated. In each case, electrical current was delivered from 0 to 220 CL in 10 CL steps. For this animal, the electrical threshold was reduced from 130 CL to 90 CL when combined with light at 75% threshold intensity, whereas the response became suprathreshold when using light at 90% of threshold. (B) The effect of sub-threshold optical intensity on the electrical threshold for hybrid channels 4 and 5 (H4 and H5) showing reduced electrical threshold at varying sub-threshold optical intensities. Individual data for each mouse is shown by a different colour ($n = 8$).

optical threshold. The average optical intensity used for H4 was 77.5% ± 2.5% ($n = 8$), and the average optical intensity used for H5 was 66.3% ± 4.5% ($n = 8$) (table 1).

Using these hybrid stimulation parameters, the change in threshold between electrical-only stimulation and hybrid stimulation was quantified for each hybrid channel in each mouse. There was a reduction in threshold with hybrid stimulation compared to electrical-only stimulation for both H4 (basal; figure 5(A)) and H5 (tip; figure 5(B)) in every case. Separate paired t-tests for H4 and H5 revealed that the changes in threshold were statistically significant at both stimulation sites (paired t-test, $p < 0.001$). The median reduction in electrical threshold for H4 was 40 CL (first quartile: 27.5 CL, third quartile 60 CL) (6 dB change) and the median reduction in electrical threshold for H5 was 55 CL (first quartile: 30 CL, third quartile 70 CL) (8.6 dB change). (figure 5(C)). The difference in the reduction of electrical threshold between the H4 and H5 channels was not significant ($p = 0.776$ paired t-test, $n = 8$).

3.3. Hybrid stimulation reduces the spread of activation

Compared to electrical stimulation (e.g. figure 2(A)), the spatial tuning curve with hybrid stimulation was sharper at low electrical stimulating currents (see figure 3(B)) but not at higher currents. The spread of activation was measured at $d' = 1$ and $d' = 2$ above the threshold for electrical and hybrid stimulation, as shown in the representative image (figure 6(A)). Analysis of the effect of stimulus modality on spread of activation indicated that the hybrid stimulation significantly reduced the activation width for both discrimination levels ($p < 0.001$). For both discrimination levels ($d' = 1$ and $d' = 2$), the spread of activation at the H4 stimulating channel was not significantly different to the spread of activation at the H5 stimulating channel ($d' = 1$, $p = 0.73$, and $d' = 2$, $p = 0.12$). This suggested that the spread of activation was independent from the stimulation site, and thus the spread of activation measured at each channel (4 and 5) was averaged for analysis of activation width. As shown in figure 6(B), the mean activation width during hybrid stimulation was approximately 1.8-fold less compared to electrical stimulation at the $d' = 1$ discrimination level, and 1.3-fold less at the $d' = 2$ discrimination level ($p < 0.05$, Two-way ANOVA, Holm-Sidak post hoc analysis). At higher stimulating currents, there is no difference in activation width between electrical and hybrid stimulation (figure 6(C)).

3.4. Simultaneous channel stimulation

Channel summation was studied by stimulating the two hybrid channels simultaneously, with the more basally positioned H4 as the interfering channel and the more apically positioned H5 as the test channel (0.52 mm pitch between H4 and H5). Sub-threshold light was used in the hybrid stimulus for this study since this is where hybrid stimulation had the most impact on the spatial tuning curve. Four different levels of electrical stimulation were added to the sub-threshold optical stimulus. Simultaneous hybrid stimulation on the two channels resulted in

Table 1. Optical intensities yielding threshold responses to optical-only stimulation for each mouse to each LED channel (L4 and L5) and the optical intensity used in hybrid stimulation for hybrid channels H4 and H5.

Mouse #	L4 threshold	Optical level used in H4	L5 threshold	Optical level used in H5
1	1.16 μW	0.93 μW (80%)	0.47 μW	0.35 μW (75%)
2	1.50 μW	1.13 μW (75%)	0.47 μW	0.35 μW (75%)
3	1.15 μW	0.81 μW (70%)	0.99 μW	0.59 μW (60%)
4	2.02 μW	1.82 μW (90%)	0.51 μW	0.43 μW (85%)
5	0.51 μW	0.41 μW (80%)	0.57 μW	0.26 μW (45%)
6	0.51 μW	0.36 μW (70%)	0.16 μW	0.10 μW (65%)
7	1.20 μW	1.02 μW (85%)	0.16 μW	0.12 μW (75%)
8	0.37 μW	0.26 μW (70%)	0.16 μW	0.08 μW (50%)
Ave.	1.05 $\pm$ 0.2 μW	0.84 μW (77.5%)	0.43 $\pm$ 0.1 μW	0.29 μW (66.3%)

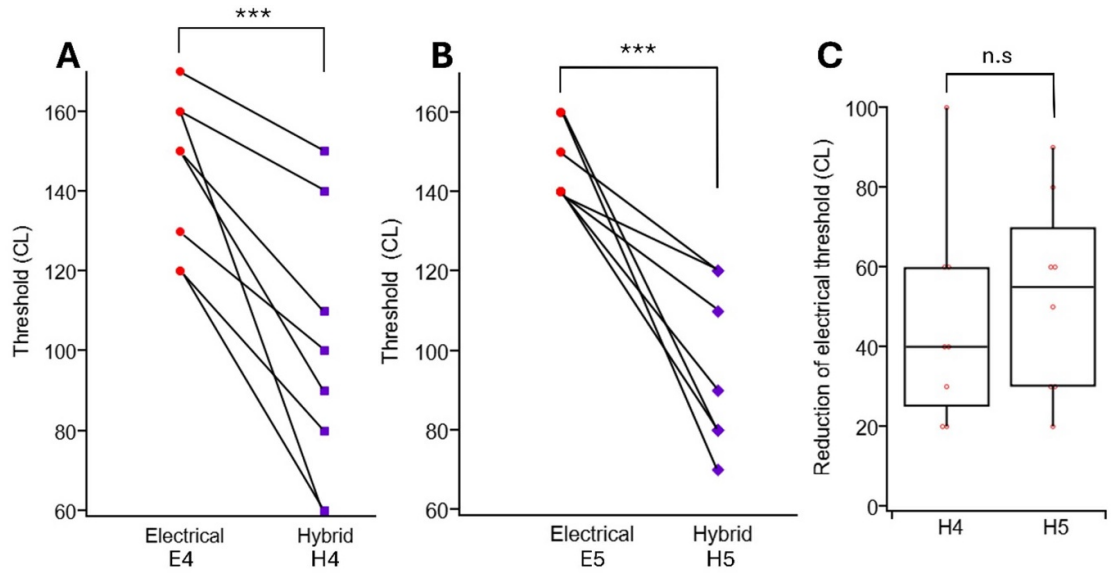

Figure 5. Comparison of electrical and hybrid stimulation threshold. (A) Threshold for the electrical-only stimulation on electrode 4 (E4) and hybrid stimulation with hybrid channel 4 (H4). (B) Threshold for the electrical-only and hybrid stimulation on electrode 5 (E5) and hybrid channel 5 (H5), respectively. In A and B, each red circle represents the electrical threshold in an individual mouse, while each purple square connected by a line represents the hybrid threshold in the same animal (same recording run; two animals had same electrical and hybrid threshold with channel 5). The data shows consistent reductions in electrical threshold during hybrid stimulation compared to electrical-only stimulation for channels 4 and 5 (paired t test, *** $p < 0.001$, $n = 8$). (C) Box plot (medians and quartiles) of the change in electrical threshold during hybrid stimulation and electrical-only stimulation for hybrid channels H4 and H5, showing no significant difference in the size of the reduction between the two channels (paired t test, $p = 0.776$, $n = 8$).

varying degrees of overlapping areas of activation, measured as a reduction in the threshold at the H5 best recording electrode (figures 7(A)–(D)). This negative threshold shift was used to measure the degree of channel interaction (i.e. the influence of the interfering channel on the test channel). Since the magnitude of the change is dependent on the threshold CL, the 'relative threshold influence' was calculated by dividing the reduction in threshold by just noticeable difference. When the hybrid H5 test channel was stimulated simultaneously with the H4 interfering channel at its subthreshold level (10 CL below threshold; Th-10), the relative threshold influence was 2.4 $\pm$ 0.9 ($n = 6$). Increasing the electrical component of the interfering channel to its threshold (Th), or 10 or 20 CL above threshold (Th + 10 and Th + 20), increased the relative threshold influence to 4.0 $\pm$ 1.3, 4.6 $\pm$ 1.8 and 8.3 $\pm$ 4.2, respectively ($n = 6$, figure 7(E)). In contrast, the level of interference observed with electrical stimulation using similar arrays and an identical experimental and analysis set up was significantly higher at all stimulating levels (two way ANOVA, $p = 0.001$, $n = 6$ per group) (figure 7(E)) (Azees *et al* 2023).

4. Discussion

The conductive nature of the cochlear perilymphatic fluid places severe limitations on the spectral resolution of electrical cochlear implants and makes simultaneous channel stimulation highly problematic. Here we present an alternative stimulation strategy that takes advantage of the high spectral resolution that can be achieved with optical stimulation (Dieter

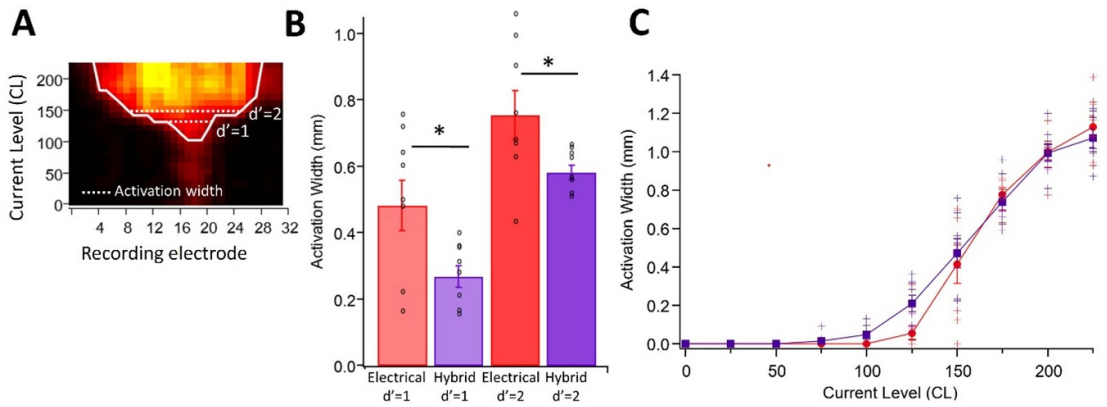

Figure 6. The activation width for monopolar electrical and hybrid stimulation. (A) A representative response image illustrating the measurement of activation width at two discrimination levels above the threshold ($d' = 1$ and $d' = 2$). (B) The mean activation width for hybrid stimulation (purple; averaged across hybrid channels 4 and 5) was significantly lower than the mean activation width for electrical stimulation (red, averaged across electrodes 4 and 5) at $d' = 1$ and $d' = 2$ above threshold (two-way ANOVA, * $p < 0.05$, $n = 8$ mice). (C) Mean activation width measured at each stimulating current level for electrical stimulation (red) and hybrid stimulation (purple). Error bars show standard error of the mean. Data from individual animals are shown as points on each chart.

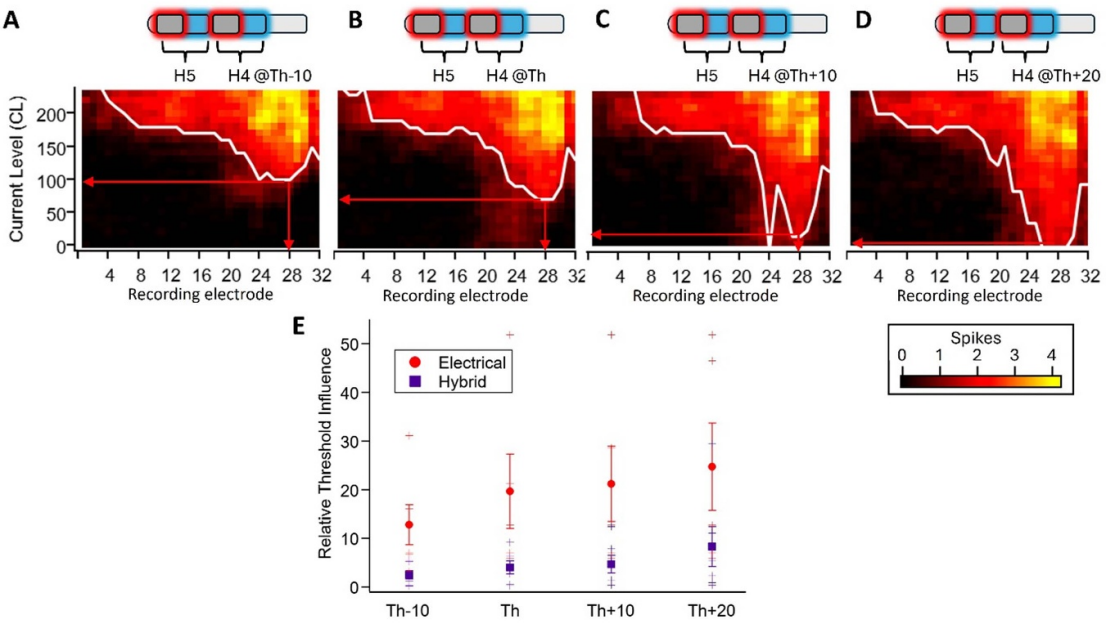

Figure 7. Simultaneous channel hybrid stimulation. (A)–(D) Response images for the simultaneous stimulation of the adjacent test H5 channel (hybrid channel 5; H5) and interfering channel (hybrid channel 4; H4) when the electrical component of the interfering channel was subthreshold (H4@Th-10 CL) (A), threshold (H4@Th) (B) or suprathreshold (H4@Th + 10 CL and H4@Th + 20 CL) (C–D). As the intensity of the interfering channel H4 was increased there was a corresponding decrease in the threshold for the test H5 best recording site (red arrows), indicating increasing interference. The spike rate at each stimulation intensity level is depicted by the colour scale. (E) Mean threshold shifts for the test H5 channel were converted to relative threshold influence by dividing the reduction in threshold by just noticeable difference (subtraction of threshold intensity from intensity at which $d' = 1$ during H5 test channel only stimulation). Electrical interference data (red) formed part of a previously published study using an electrical array with electrodes of similar pitch (0.6 mm pitch for electrical array compared to 0.52 mm pitch for hybrid array) (Azees *et al* 2023) and are included here for comparison with the hybrid interference data. There was a significantly less interference during hybrid stimulation (purple) compared to electrical stimulation at all interfering channel intensities (two-way ANOVA, $p = 0.001$, $n = 6$). Error bars show the standard error of the mean. Data from individual animals are shown as points on each chart.

et al 2019, Keppeler *et al* 2020), made possible via optogenetics. A key advantage of combining optical stimulation with electrical stimulation, rather than using optical stimulation alone, is the improvement in the reliability of responses during rapid pulsed stimulation, particularly when using near-threshold light in the combined stimulus (Thompson *et al* 2020, Ajay *et al* 2023, 2024). However, these studies did not use translatable methods of delivering light and electrical stimuli to the spiral ganglion neurons. Here, we expand these findings to a multichannel hybrid device that more closely models a clinical cochlear

implant, allowing us to examine spread of activation and channel summation during simultaneous hybrid stimulation, which has not been explored previously. Our results demonstrate a significant reduction in the spread of activation and channel summation during hybrid stimulation compared to electrical-only stimulation when measured at $d' = 1$ and $d' = 2$ above threshold, but not at higher stimulating currents. However, it should be noted that channel summation comparisons between electrical and hybrid stimulation were in different animals and across studies and would more ideally be compared in the same animal. It is difficult to determine how the benefits of hybrid stimulation at these suprathreshold levels of spiking activity relate to loudness, hence interpreting the clinical impact is difficult. Clinical electrical stimulation in animal models have shown that audible levels are within the range of electrical auditory brainstem response (EABR) threshold −3 dB to EABR threshold +6 dB (Irving *et al* 2014). This suggests that the hybrid approach may offer improved spectral selectivity and response reliability at higher rate stimulation in some conditions (e.g. in quiet), which is crucial for enhancing speech perception or music appreciation outcomes in cochlear implant recipients.

We developed a hybrid cochlear implant for the mouse cochlea by adding 0.059 mm2 LEDs to an array of platinum electrodes closely resembling those used in human full-ring cochlear implants, with tapering diameter to facilitate insertion. The LEDs were incorporated into the array such that they alternated with the platinum electrodes. The 270 × 220 μm LEDs were fabricated on thin film polyimide with 0.52 mm pitch to comfortably accommodate the 200 μm length platinum rings. It was necessary to coat the thin film LEDs with parylene C for moisture protection and increased durability. This step was performed prior to integration with the electrodes, so that plasma etching or laser ablation processes were not required to expose the electrode surface. The parylene C coating did not significantly alter the power output, demonstrating suitable transparency of the encapsulation layers. The power output was sufficient for activation of the ChR2-H134R opsin expressed in the spiral ganglion neurons of ChR2-H134R heterozygous transgenic mice, although it is known that expression levels can impact optical thresholds, either by the number of cells transduced (Richardson *et al* 2021) or level of expression within each cell (Meng *et al* 2019). Considering the specified LED currents, pulse duration, and repetition rate, any effects attributed to tissue heating were expected to be negligible (Zgierski-Johnston *et al* 2020). While it was possible to fully insert the hybrid array into the mouse cochlea, full insertion often caused mechanical stress, resulting in failure of the conformal coating. Further reduction in size or flexibility of hybrid arrays will be necessary to minimise mechanical stress during deeper insertions. Given the intended lifespan of these devices (ideally a lifetime), the components must exhibit exceptional operational stability, biocompatibility, and flexibility within the cochlear environment. Parylene/silicone combinations offer a promising solution for protection, flexibility, and optical properties, are approved materials by the Food and Drug Administration, and are in clinical use in implanted Utah and retinal arrays (Roessler *et al* 2009, Normann *et al* 2016), but long-term testing in the cochlear setting is still needed.

During optical-only stimulation of optogenetically modified animals, the spread of activation and interaction between simultaneous channel stimulation is significantly lower compared to electrical-only stimulation, even at high stimulating intensities (Dieter *et al* 2019, Keppeler *et al* 2020, Azees *et al* 2023). Combining sub-threshold electrical and sub/near-threshold optical stimulation improved the reliability of responses at higher rates (>100 Hz) without greatly impacting spectral resolution (Thompson *et al* 2020, Ajay *et al* 2023). The maintained spectral resolution of hybrid stimulation is due to facilitation between the optical and electrical stimuli, reducing the electrical current required to achieve threshold activation. This effect has also been demonstrated in the sciatic nerve (Duke *et al* 2012a, 2012b, Matarazzo *et al* 2023). An additional benefit of the sub-threshold optical levels used in hybrid stimulation (e.g. ∼75% of optical threshold as used here), is the reduced power consumption compared to optical-only strategies, which are currently higher than electrical-only solutions (Hernandez *et al* 2014, Richardson *et al* 2020). Our data supports previous studies on hybrid stimulation in the cochlea, but with several key differences. Previously, the direction of the light stimulus was not optimised to the spiral ganglion as it was constrained by the fibre optic insertion into the scala tympani, leading to a much broader area of activation compared to the findings in this study (Thompson *et al* 2020). Here, and in a related study on optical-only stimulation (Azees *et al* 2023), we stimulated with multichannel arrays that directed the light towards the spiral ganglion neurons. Conversely, the spread of the electrical stimulus in the Thompson study was unusually narrow as it was delivered by a 25 μm platinum wire where both size and geometry may impact current spread, whereas the electrical stimuli in the Azees and present studies were delivered by electrodes modelled on the clinical cochlear implant. Finally, whereas hybrid stimulation was previously limited to a single channel, here we were able to perform hybrid stimulation at two distinct locations in the cochlea.

The results of this study can be directly compared to our previous work on multi-channel LED stimulation. Both studies were conducted using a similar experimental design, including the use of the same

transgenic mouse model, the same method of acute deafening, and identical LED fabrication method. The activation width for hybrid stimulation at $d' = 1$ and $d' = 2$ above threshold in this study was 22% and 52% higher than the activation width measured during optical-only stimulation measured previously (0.22 ± 0.04 mm and 0.38 ± 0.04 mm at $d' = 1$ and 2 respectively) using LED arrays with the same pitch of 0.52 mm (Azees *et al* 2023). Hence, compared to optical-only stimulation, hybrid stimulation markedly broadened out at the higher stimulating currents.

It is well known that spread of activation results in the number of independent stimulating channels being lower than the actual number of cochlear implant electrodes. This negatively impacts speech recognition with the cochlear implant (Goehring *et al* 2021, Cychosz *et al* 2022). Friesen *et al* reported that individuals with the highest level of speech intelligibility typically have around seven independent channels. However, for individuals with low levels of speech recognition, the number of independent channels was only four (2001). Increasing the number of independent channels by reducing spread of activation would undoubtedly benefit cochlear implant recipients. Here, channel summation during simultaneous stimulation was assessed by measuring threshold shifts on the best recording electrode in the ICs, consistent with prior studies evaluating interactions between simultaneous electrical channels (Bierer 2007, Middlebrooks *et al* 2007, George *et al* 2015). We previously showed that channel interactions during simultaneous optical-only stimulation was significantly lower than simultaneous electrical stimulation using the same transgenic mouse model, LEDs, and electrodes used here (Azees *et al* 2023). It is noteworthy that the relative threshold influence was significantly lower for hybrid stimulation (using electrodes with 0.52 mm pitch) as compared to electrical-only stimulation (0.6 mm pitch) in the previous study, and not significantly different to optical stimulation, using the same experimental setup. While we previously investigated optical- and electrical-only channel interactions at various inter-electrode spacings, in this study we could only use adjacent channels for simultaneous hybrid stimulation, where interference is highest. Moving forward, channel interactions during hybrid stimulation should be measured at different inter-electrode spacings. It should be noted that, due to the broad current spread from electrodes at higher stimulating currents, each LED is likely to create a hybrid channel with neighbouring as well as more distant electrodes. Future research could explore current steering, a technique used in retinal prostheses (Dumm *et al* 2014, Meikle *et al* 2022, Wu *et al* 2023) and cochlear implants (Firszt *et al* 2007, Koch *et al* 2007, Berenstein *et al* 2008, Frijns *et al* 2009, Donaldson *et al* 2011), to manipulate the distribution of electrical current and improve the overlap of the optical and electrical elements of the hybrid stimulus, thus localising a hybrid channel more effectively.

A transgenic mouse model in which all neurons were transfected with ChR2-H134R were used for this study to test the optogenetic/hybrid stimulation. However, in clinical applications, opsin needs to be introduced using a viral vector and consequently may not be expressed in all neurons. Recent studies suggest that hybrid stimulation may not be as effective in non-transgenic models compared to transgenic mice (Richardson *et al* 2021, Ajay *et al* 2023, 2024). This was partially attributed to poor overlap between the optical and electrical stimuli, which may be further exacerbated in hybrid arrays with alternately arranged electrodes and LEDs. Again, current steering across two electrodes on either side of an LED could help by creating a virtual channel that overlies the LED for maximal stimulation of that region. It will be crucial to verify the spatial precision and channel interactions in AAV-injected mice. Furthermore, additional research will be needed to determine the applicability of these findings to animals with chronic deafness, where loss of spiral ganglion neurons may influence outcomes (Ajay *et al* 2023), and in chronically implanted and stimulated animals, where factors such as fibrous tissue formation around the implanted array (Kawano *et al* 1998, Seyyedi *et al* 2014, Fallon *et al* 2022) may influence the delivery of the optical and electrical stimuli to the neurons. It should also be acknowledged that many factors may influence how these results translate to humans, including geometric differences between species, the relative size of the electrode compared to the neurons, the use of single pulses versus pulse trains, single electrode stimulation versus masker probe paradigms in humans, the difference in neural health between species, and differences in temporal dynamics at the auditory nerve. Hence, while the results suggest a potential benefit of our approach, a raft of additional research will be required before any clinical deployment can be considered.

The findings of our study shed light on the potential benefits and limitations of combining electrical and optogenetic stimulation in a multi-channel system. Less interaction between channels suggests a potential advantage of hybrid stimulation and enable simultaneous multi-channel stimulation, but these advantages would be lost at higher electrical stimulation levels. Simultaneous stimulation across multiple channels could increase the performance of cochlear implants by allowing for better representation of complex sounds, such as speech and music, by encoding different frequency components simultaneously. Cochlear implant users could potentially perceive more natural and detailed auditory cues, leading to improved speech and music perception.

5. Conclusion

Hybrid stimulation uses sub-threshold levels of light to help depolarise the spiral ganglion neurons in a spatially restricted region of the cochlea prior to the delivery of the electrical stimulus. Since the light lowers the level of electrical stimulation needed for activation in the region of the LED, the overall spread of activation is low compared to electrical-only stimulation at low stimulating currents. In addition, hybrid stimulation has been shown previously to improve reliability at higher stimulation rates compared to optical-only stimulation. Here, we have shown that while the spatial precision of hybrid stimulation lies between that of optical and electrical stimulation, it is still significantly more precise compared to electrical-only stimulation at the two measured suprathreshold levels. We further establish the independence of adjacent stimulation channels through analysis of thresholds at stimulating sites. In line with the high spectral resolution of hybrid stimulation using sub-threshold optical and electrical stimuli, there was little interaction even at channel pitch of 0.52 mm, potentially allowing the simultaneous stimulation of multiple channels independently for enhanced speech perception. This hybrid stimulation approach, utilising the precision of optical stimulation while exploiting electrical stimulation to improve temporal responses, would enhance encoding of complex speech signals as well as the fine changes in the timing information of speech.

Data availability statement

The data cannot be made publicly available upon publication because no suitable repository exists for hosting data in this field of study. The data that support the findings of this study are available upon reasonable request from the authors.

Acknowledgment

This work was supported by the National Health and Medical Research Council of Australia (Grant #2002523). Ajmal Azees was supported by a joint scholarship between the Bionics Institute and RMIT University. The Bionics Institute acknowledges the support it receives from the Victorian Government through its Operational Infrastructure Support Program.

Author contributions

Conception and study design: R R, J F, A A. Data collection and analysis: A A, J F, A T. Data interpretation, manuscript writing and editing: All authors.

ORCID iDs

Ajmal A Azees https://orcid.org/0000-0001-9044-5828
Alex C Thompson https://orcid.org/0000-0002-8012-872X
Patrick Ruther https://orcid.org/0000-0002-7358-003X
Elise A Ajay https://orcid.org/0000-0002-7422-4934
Ulises A Aregueta Robles https://orcid.org/0000-0001-9162-465X
David J Garrett https://orcid.org/0000-0002-4676-8387
James B Fallon https://orcid.org/0000-0003-2686-3886
Rachael T Richardson https://orcid.org/0000-0002-2412-8354

References

Ajay E A, Thompson A C, Azees A A, Wise A K, Grayden D B, Fallon J B and Richardson R T 2024 Combined-electrical optogenetic stimulation but not channelrhodopsin kinetics improves the fidelity of high rate stimulation in the auditory pathway in mice *Sci. Rep.* **14** 21028
Ajay E A, Trang E P, Thompson A C, Wise A K, Grayden D B, Fallon J B and Richardson R T 2023 Auditory nerve responses to combined optogenetic and electrical stimulation in chronically deaf mice *J. Neural Eng.* **20** 026035
Albert E S *et al* 2012 TRPV4 channels mediate the infrared laser-evoked response in sensory neurons *J. Neurophysiol.* **107** 3227–34
Aregueta Robles U A, Bartlett-Tomasetig F and Poole-Warren L A 2023 Growing human-scale scala tympani-likein vitrocell constructs *Biofabrication* **15** 035014
Azees A A *et al* 2023 Spread of activation and interaction between channels with multi-channel optogenetic stimulation in the mouse cochlea *Hear Res.* **440** 108911
Berenstein C K, Mens L H, Mulder J J and Vanpoucke F J 2008 Current steering and current focusing in cochlear implants: comparison of monopolar, tripolar, and virtual channel electrode configurations *Ear Hear* **29** 250–60
Bierer J A 2007 Threshold and channel interaction in cochlear implant users: evaluation of the tripolar electrode configuration *J. Acoust. Soc. Am.* **121** 1642–53
Bierer J A and Middlebrooks J C 2002 Auditory cortical images of cochlear-implant stimuli: dependence on electrode configuration *J. Neurophysiol.* **87** 478–92
Bierer J A and Middlebrooks J C 2004 Cortical responses to cochlear implant stimulation: channel interactions *J. Assoc. Res. Otolaryngol.* **5** 32–48
Black R C, Clark G M and Patrick J F 1981 Current distribution measurements within the human cochlea *IEEE Trans. Biomed. Eng.* **28** 721–5
Crane R, Conley S M, Al-Ubaidi M R and Naash M I 2021 Gene therapy to the retina and the cochlea *Front. Neurosci.* **15** 652215
Cychosz M, Xu K and Fu Q-J 2022 Effects of spectral smearing on speech understanding and masking release in simulated bilateral cochlear implants *J. Acoust. Soc. Am.* **152** A141
Deisseroth K 2011 Optogenetics *Nat. Methods* **8** 26–29
Deisseroth K 2015 Optogenetics: 10 years of microbial opsins in neuroscience *Nat. Neurosci.* **18** 1213–25
Dieter A *et al* 2020b muLED-based optical cochlear implants for spectrally selective activation of the auditory nerve *EMBO Mol. Med.* **12** e12387

Dieter A, Duque-Afonso C J, Rankovic V, Jeschke M and Moser T 2019 Near physiological spectral selectivity of cochlear optogenetics *Nat. Commun.* **10** 1962

Dieter A, Keppeler D and Moser T 2020a Towards the optical cochlear implant: optogenetic approaches for hearing restoration *EMBO Mol. Med.* **12** e11618

Dombrowski T, Rankovic V and Moser T 2019 Toward the optical cochlear implant *Cold Spring Harbor Perspect. Med.* **9** a033225

Donaldson G S, Dawson P K and Borden L Z 2011 Within-subjects comparison of the HiRes and Fidelity120 speech processing strategies: speech perception and its relation to place-pitch sensitivity *Ear Hear* **32** 238–50

Duke A R, Cayce J M, Malphrus J D, Konrad P, Mahadevan-Jansen A and Jansen E D 2009 Combined optical and electrical stimulation of neural tissue in vivo *J. Biomed. Opt.* **14** 060501

Duke A R, Lu H, Jenkins M W, Chiel H J and Jansen E D 2012a Spatial and temporal variability in response to hybrid electro-optical stimulation *J. Neural Eng.* **9** 036003

Duke A R, Peterson E, Mackanos M A, Atkinson J, Tyler D and Jansen E D 2012b Hybrid electro-optical stimulation of the rat sciatic nerve induces force generation in the plantarflexor muscles *J. Neural Eng.* **9** 066006

Dumm G, Fallon J B, Williams C E and Shivdasani M N 2014 Virtual electrodes by current steering in retinal prostheses *Invest. Ophthalmol. Vis. Sci.* **55** 8077–85

Fallon J B, Dueck W, Trang E P, Smyth D and Wise A K 2022 Effects of chronic implantation and long-term stimulation of a cochlear implant in the partial hearing cat model *Hear. Res.* **426** 108470

Fenno L, Yizhar O and Deisseroth K 2011 The development and application of optogenetics *Annu. Rev. Neurosci.* **34** 389–412

Fielden C A, Kluk K, Boyle P J and McKay C M 2015 The perception of complex pitch in cochlear implants: a comparison of monopolar and tripolar stimulation *J. Acoust. Soc. Am.* **138** 2524–36

Firszt J B, Koch D B, Downing M and Litvak L 2007 Current steering creates additional pitch percepts in adult cochlear implant recipients *Otol. Neurotol.* **28** 629–36

Friesen L M, Shannon R V, Baskent D and Wang X 2001 Speech recognition in noise as a function of the number of spectral channels: comparison of acoustic hearing and cochlear implants *J. Acoust. Soc. Am.* **110** 1150–63

Frijns J H, Kalkman R K, Vanpoucke F J, Bongers J S and Briaire J J 2009 Simultaneous and non-simultaneous dual electrode stimulation in cochlear implants: evidence for two neural response modalities *Acta Otolaryngol.* **129** 433–9

Fu Q J 2002 Temporal processing and speech recognition in cochlear implant users *Neuroreport* **13** 1635–9

Fu Q J and Nogaki G 2005 Noise susceptibility of cochlear implant users: the role of spectral resolution and smearing *J. Assoc. Res. Otolaryngol.* **6** 19–27

Fu Q J and Shannon R V 2000 Effect of stimulation rate on phoneme recognition by nucleus-22 cochlear implant listeners *J. Acoust. Soc. Am.* **107** 589–97

Fu Q J, Shannon R V and Wang X 1998 Effects of noise and spectral resolution on vowel and consonant recognition: acoustic and electric hearing *J. Acoust. Soc. Am.* **104** 3586–96

George S S, Shivdasani M N, Wise A K, Shepherd R K and Fallon J B 2015 Electrophysiological channel interactions using focused multipolar stimulation for cochlear implants *J. Neural Eng.* **12** 066005

George S S, Wise A K, Shivdasani M N, Shepherd R K and Fallon J B 2014 Evaluation of focused multipolar stimulation for cochlear implants in acutely deafened cats *J. Neural Eng.* **11** 065003

Gfeller K, Turner C, Oleson J, Zhang X, Gantz B, Froman R and Olszewski C 2007 Accuracy of cochlear implant recipients on pitch perception, melody recognition, and speech reception in noise *Ear Hearing* **28** 412–23

Goehring T, Archer-Boyd A W, Arenberg J G and Carlyon R P 2021 The effect of increased channel interaction on speech perception with cochlear implants *Sci. Rep.* **11** 10383

Green D M and Swets J A 1973 *Signal Detection Theory and Psychophysics* (R. E. Krieger Pub. Co)

Heffer L F and Fallon J B 2008 A novel stimulus artifact removal technique for high-rate electrical stimulation *J. Neurosci. Methods* **170** 277–84

Helke C, Reinhardt M, Arnold M, Schwenzer F, Haase M, Wachs M, Goßler C, Götz J, Keppeler D and Wolf B 2022 On the fabrication and characterization of polymer-based waveguide probes for use in future optical cochlear implants *Materials* **16** 106

Hernandez V H *et al* 2014 Optogenetic stimulation of the auditory pathway *J. Clin. Investig.* **124** 1114–29

Huang C-Y, Yang H-M, Sher Y-J, Lin Y-H and Wu J-L 2005 Speech intelligibility of Mandarin-speaking deaf children with cochlear implants *Int. J. Pediatric Otorhinolaryngol.* **69** 505–11

Huet A, Mager T, Gossler C and Moser T 2024 Toward optogenetic hearing restoration *Annu. Rev. Neurosci.* **47** 103–21

Irving S, Wise A K, Millard R E, Shepherd R K and Fallon J B 2014 A partial hearing animal model for chronic electro-acoustic stimulation *J. Neural Eng.* **11** 046008

Jürgens T, Hohmann V, Büchner A and Nogueira W 2018 The effects of electrical field spatial spread and some cognitive factors on speech-in-noise performance of individual cochlear implant users—A computer model study *PLoS One* **13** e0193842

Kawano A, Seldon H L, Clark G M, Ramsden R T and Raine C H 1998 Intracochlear factors contributing to psychophysical percepts following cochlear implantation *Acta Otolaryngol.* **118** 313–26

Keppeler D *et al* 2018 Ultrafast optogenetic stimulation of the auditory pathway by targeting-optimized Chronos *EMBO J.* **37** e99649

Keppeler D *et al* 2020 Multichannel optogenetic stimulation of the auditory pathway using microfabricated LED cochlear implants in rodents *Sci. Transl. Med.* **12** eabb8086

Keppeler D *et al* 2021 Multiscale photonic imaging of the native and implanted cochlea *Proc. Natl Acad. Sci.* **118** e2014472118

Khurana L, Harczos T, Moser T and Jablonski L 2023 En route to sound coding strategy for optical cochlear implants *Iscience* **26** 107725

Khurana L, Keppeler D, Jablonski L and Moser T 2022 Model-based prediction of optogenetic sound encoding in the human cochlea by future optical cochlear implants *Comput. Struct. Biotechnol. J.* **20** 3621–9

Klein E, Kaku Y, Paul O and Ruther P 2019 Flexible μLED-based optogenetic tool with integrated μ-lens array and conical concentrators providing light extraction improvements above 80% *2019 IEEE 32nd Int. Conf. on Micro Electro Mechanical Systems (MEMS)* (IEEE)

Koch D B, Downing M, Osberger M J and Litvak L 2007 Using current steering to increase spectral resolution in CII and HiRes 90K users *Ear Hear* **28** 38S–41S

Kral A, Hartmann R, Mortazavi D and Klinke R 1998 Spatial resolution of cochlear implants: the electrical field and excitation of auditory afferents *Hear Res.* **121** 11–28

Lehnhardt E, Gnadeberg D, Battmer R and Von Wallenberg E 1992 Experience with the cochlear miniature speech processor in adults and children together with a comparison of unipolar and bipolar modes *ORL* **54** 308–13

Lin J Y 2011 A user's guide to channelrhodopsin variants: features, limitations and future developments *Exp. Physiol.* **96** 19–25

Mager T *et al* 2018 High frequency neural spiking and auditory signaling by ultrafast red-shifted optogenetics *Nat. Commun.* **9** 1750

Marozeau J, McDermott H J, Swanson B A and McKay C M 2015 Perceptual interactions between electrodes using focused

and monopolar cochlear stimulation *J. Assoc. Res. Otolaryngol.* **16** 401–12
Matarazzo J V, Ajay E A, Payne S C, Trang E P, Thompson A C, Marroquin J B, Wise A K, Fallon J B and Richardson R T 2023 Combined optogenetic and electrical stimulation of the sciatic nerve for selective control of sensory fibers *Front. Neurosci.* **17** 1190662
McDermott H J 2004 Music perception with cochlear implants: a review *Trends. Amplif.* **8** 49–82
Meikle S J, Hagan M A, Price N S and Wong Y T 2022 Intracortical current steering shifts the location of evoked neural activity *J. Neural Eng.* **19** 035003
Meng X, Murali S, Cheng Y, Lu J, Hight A E, Kanumuri V V, Brown M C, Holt J R, Lee D J and Edge A S B 2019 Increasing the expression level of ChR2 enhances the optogenetic excitability of cochlear neurons *J. Neurophysiol.* **122** 1962–74
Mens L H and Berenstein C K 2005 Speech perception with mono-and quadrupolar electrode configurations: a crossover study *Otol. Neurotol.* **26** 957–64
Middlebrooks J C and Snyder R L 2007 Auditory prosthesis with a penetrating nerve array *J. Assoc. Res. Otolaryngol.* **8** 258–79
Mittring A, Moser T and Huet A T 2023 Graded optogenetic activation of the auditory pathway for hearing restoration *Brain Stimul.* **16** 466–83
Moser T 2022 Restoring hearing with beams of light *IEEE Spectr.* **59** 30–35
Normann R A and Fernandez E 2016 Clinical applications of penetrating neural interfaces and Utah Electrode Array technologies *J. Neural Eng.* **13** 061003
Pfingst B E, Franck K H, Xu L, Bauer E M and Zwolan T A 2001 Effects of electrode configuration and place of stimulation on speech perception with cochlear prostheses *J. Assoc. Res. Otolaryngol.* **2** 87
Pfingst B E, Zwolan T A and Holloway L A 1997 Effects of stimulus configuration on psychophysical operating levels and on speech recognition with cochlear implants *Hearing Res.* **112** 247–60
Poursoroush S, Ghorbani A, Soleymani Z, Kamali M, Yousefi N and Poursoroush Z 2015 Speech intelligibility of cochlear-implanted and normal-hearing children *Iranian J. Otorhinolaryngol.* **27** 361 (available at: https://pmc.ncbi.nlm.nih.gov/articles/PMC4639689/)
Qi J, Fu X, Zhang L, Tan F, Li N, Sun Q, Hu X, He Z, Xia M and Chai R 2022 Current AAV-mediated gene therapy in sensorineural hearing loss *Fundam. Res.* **5** 192–202
Quass G L and Kral A 2024 Tripolar configuration and pulse shape in cochlear implants reduce channel interactions in the temporal domain *Hear Res.* **443** 108953
Richardson R T, Ibbotson M R, Thompson A C, Wise A K and Fallon J B 2020 Optical stimulation of neural tissue *Healthcare Technol. Lett.* **7** 58–65
Richardson R T, Thompson A C, Wise A K, Ajay E A, Gunewardene N, O'Leary S J, Stoddart P R and Fallon J B 2021 Viral-mediated transduction of auditory neurons with opsins for optical and hybrid activation *Sci. Rep.* **11** 11229
Roessler G *et al* 2009 Implantation and explantation of a wireless epiretinal retina implant device: observations during the EPIRET3 prospective clinical trial *Invest Ophthalmol. Vis. Sci.* **50** 3003–8
Seyyedi M and Nadol J B Jr 2014 Intracochlear inflammatory response to cochlear implant electrodes in humans *Otol. Neurotol.* **35** 1545–51
Shannon R V 1983 Multichannel electrical stimulation of the auditory nerve in man. II. Channel interaction *Hear Res.* **12** 1–16
Shannon R V, Fu Q-J and Galvin J 2004 The number of spectral channels required for speech recognition depends on the difficulty of the listening situation *Acta Oto-Laryngologica* **124** 50–54
Snyder R L, Bierer J A and Middlebrooks J C 2004 Topographic spread of inferior colliculus activation in response to acoustic and intracochlear electric stimulation *J. Assoc. Res. Otolaryngol.* **5** 305–22
Srinivasan A G, Padilla M, Shannon R V and Landsberger D M 2013 Improving speech perception in noise with current focusing in cochlear implant users *Hear Res.* **299** 29–36
Stevens S M, Brown L N, Ezell P C and Lang H 2015 The mouse round-window approach for ototoxic agent delivery: a rapid and reliable technique for inducing cochlear cell degeneration *J. Vis. Exp.* **105** 53131
Thompson A C, Wise A K, Hart W L, Needham K, Fallon J B, Gunewardene N, Stoddart P R and Richardson R T 2020 Hybrid optogenetic and electrical stimulation for greater spatial resolution and temporal fidelity of cochlear activation *J. Neural Eng.* **17** 056046
WHO 2021 Deafness and hearing loss (available at: ww.who.int/health-topics/hearing-loss#tab=tab_1) (Accessed 14 July 2021)
Wilson B S and Dorman M F 2008 Cochlear implants: a remarkable past and a brilliant future *Hear Res.* **242** 3–21
Wrobel C, Dieter A, Huet A, Keppeler D, Duque-Afonso C J, Vogl C, Hoch G, Jeschke M and Moser T 2018 Optogenetic stimulation of cochlear neurons activates the auditory pathway and restores auditory-driven behavior in deaf adult gerbils *Sci. Transl. Med.* **10** eaao0540
Wu K Y, Mina M, Sahyoun J-Y, Kalevar A and Tran S D 2023 Retinal prostheses: engineering and clinical perspectives for vision restoration *Sensors* **23** 5782
Yoshimura H, Nishio S Y and Usami S I 2021 Milestones toward cochlear gene therapy for patients with hereditary hearing loss *Laryngoscope Investigative Otolaryngol.* **6** 958–67
Zerche M, Wrobel C, Kusch K, Moser T and Mager T 2023 Channelrhodopsin fluorescent tag replacement for clinical translation of optogenetic hearing restoration *Mol. Ther. Methods Clin. Dev.* **29** 202–12
Zgierski-Johnston C M, Ayub S, Fernández M, Rog-Zielinska E, Barz F, Paul O, Kohl P and Ruther P 2020 Cardiac pacing using transmural multi-LED probes in channelrhodopsin-expressing mouse hearts *Prog. Biophys. Mol. Biol.* **154** 51–61
Zhang W, Kim S M, Wang W, Cai C, Feng Y, Kong W and Lin X 2018 Cochlear gene therapy for sensorineural hearing loss: current status and major remaining hurdles for translational success *Front. Mol. Neurosci.* **11** 221
Zwolan T A, Kileny P R, Ashbaugh C and Telian S A 1996 Patient performance with the Cochlear Corporation "20 + 2" implant: bipolar versus monopolar activation *Am. J. Otol.* **17** 717–23 (available at: www.ncbi.nlm.nih.gov/entrez/query.fcgi?cmd=Retrieve&db=PubMed&dopt=Citation&list_uids=8892567)